Available online at www.sciencedirect.com
SCIENCE DIRECT®
Journal of Crystal Growth 266 (2004) 481–486
JOURNAL OF CRYSTAL GROWTH
www.elsevier.com/locate/jcrysgro

Effect of rhodium doping on the growth and characteristics of $BaTiO_3$ single crystals grown by step-cooling method

S. Madeswaran[a], N.V. Giridharan[a], R. Varatharajan[b], G. Ravi[c], R. Jayavel[a,*]

[a] *Crystal Growth Centre, Anna University, Sardar Patel Road, Chennai 600 025, India*
[b] *Cermet Inc., Atlanta, GA 30318, USA*
[c] *National Institute for Materials Science, Tsukuba 305-0044, Japan*

Received 1 March 2003; accepted 5 March 2004
Communicated by M. Schieber

Abstract

Single crystals of Rh-doped $BaTiO_3$ have been grown by high-temperature solution growth technique. The dopant has significant effect on the growth parameters and crystal properties. Bulk single crystals of dimensions $5 \times 5 \times 4\,mm^3$ have been grown with optimized growth conditions. Layer growth and vein-like structure patterns, indicative of 2D-nucleation mechanism, have been observed on the grown crystals. The dopant level in the grown crystals was estimated by EDX analysis. The crystals possess tetragonal structure and the tetragonality decreases for higher dopant concentration. Rh doping in $BaTiO_3$ leads to decrease in dielectric constant and Curie temperature (T_c) values.

PACS: 77.84.−s; 77.80.−e; 77.22.Ch; 77.80.Dj; 74.25.Gz

Keywords: A2. High temperature solution growth; B2. Ferroelectric materials

1. Introduction

Photorefractive materials (PRs) are of great interest owing to their large non-linear response under relatively low intensity illumination [1]. In the IR and near IR regions, these materials find useful applications such as diode laser beam combining, injection-locking semiconductor diode arrays, correcting semiconductor laser modes using phase-conjugating mirrors and brightness enhancement [2]. Barium titanate doped with rhodium (Rh:$BaTiO_3$) is a potential photorefractive material in the IR and near IR regions [3]. Barium titanate crystal has been studied for its potential use in optical data storage and optical computing applications. In $BaTiO_3$, the photorefractive effect and stimulated photorefractive scattering can be realized without the application of high electric fields, which is normally required for other materials [4]. The major limitation in the performance of $BaTiO_3$ is its slow response time. Attempts have been made to decrease the response time by doping Rh in $BaTiO_3$ single crystal while maintaining the photorefractive gain, and thus

*Corresponding author. Tel.: +914422203571; fax: +914422352870.
E-mail address: rjvel@annauniv.edu (R. Jayavel).

0022-0248/$ - see front matter © 2004 Elsevier B.V. All rights reserved.
doi:10.1016/j.jcrysgro.2004.03.004

improving its viability for optical information processing applications [5,6]. It has been reported that self-pumped phase conjugation (SPPC) in Rh:$BaTiO_3$ is strongly influenced by the dopant concentration [7,8]. An efficient photorefractive ring resonator has been realized using Rh:$BaTiO_3$ with low absorption coefficient [9]. Crystals of higher Rh concentration (2000–5000 ppm) are essential in order to achieve a low absorption coefficient with high two-beam coupling gain [10].

The photo-refractive properties, SPPC and near-infrared absorption for different levels of Rh in $BaTiO_3$ have already been studied [9–11]. However, the effect of Rh dopant on the crystal growth kinetics and ferroelectric properties has not been studied. In this investigation, growth aspects of Rh-doped $BaTiO_3$ with higher dopant concentration have been studied. In view of the fact that the segregation coefficient of Rh in $BaTiO_3$ is very low [10], in the present study, the starting dopant concentration was taken in mol%, namely 1, 3 and 5 mol%. Growth of bulk crystals of Rh:$BaTiO_3$ is difficult owing to the inherent nature of twin formation, especially for higher dopant concentration. Hence a step-cooling method has been adapted to growth bulk single crystals. Effect of Rh-doping on the growth parameters has been systematically studied and bulk crystals have been grown with optimized growth conditions. Domain patterns, structural and ferroelectric properties of the grown crystals have also been studied.

2. Experiments

Rh:$BaTiO_3$ precursor was synthesized using the starting materials of high purity $BaCO_3$ (99.98%), TiO_2 (99.99%) and Rh (99.9%) by calcination at 1000°C for 10–12 h with different doping levels (1, 3 and 5 mol%). The calcined powder was taken in a 100 cc platinum crucible and mixed with KF flux in the required flux–charge ratio. The crucible was tightly closed by platinum lid to avoid the evaporation of KF and loaded into a vertical type resistively heated furnace controlled by a Eurotherm (model 818) temperature controller with an accuracy of ± 1°C. Bulk crystals were grown by step-cooling process using the following temperature cycle:

$$\mathrm{RT} \xrightarrow{75^\circ\mathrm{C/h}} 1170-1200^\circ\mathrm{C} \xrightarrow{10-15\ \mathrm{h}} 1170-1200^\circ\mathrm{C}$$

$$\xrightarrow{1^\circ\mathrm{C/h}} 1050^\circ\mathrm{C} \xrightarrow{2^\circ\mathrm{C/h}} 900^\circ\mathrm{C}$$

$$\xrightarrow{3-5^\circ\mathrm{C/h}} 800^\circ\mathrm{C} \xrightarrow{50^\circ\mathrm{C/h}} \mathrm{RT}$$

The furnace was heated up to 1170–1200°C depending on the dopant concentration, homogenized for 10–15 h and then slowly cooled to 1050°C at a rate of 1°C/h followed by an intermediate soaking for 5–10 h. Subsequently, the melt was cooled to 900°C at a rate of 2°C/h and then to 800°C at 3–5°C/h followed by a fast cooling (50°C/h) to room temperature. After a typical growth period of 10 days, the grown crystals were separated from the flux by dissolving in hot distilled water. Growth parameters, like flux–charge ratio, cooling rate and soaking period were optimized from successive growth runs. Crystals were grown for three different dopant concentrations (1, 3 and 5 mol%). Growth mechanism and surface morphology of the grown crystals were studied using an optical microscope in the reflection mode. Powder XRD patterns were recorded by using X-ray diffractometer with Fe ($\lambda = 1.9373$ Å) radiation. Chemical composition was estimated by the EDX analysis. For dielectric measurements, silver electrodes were formed on the crystal surface and the study was performed from room temperature to 200°C using HP 4194 A impedance/gain-phase analyzer at different frequencies.

3. Result and discussion

For lower doping concentration (1 mol%), butterfly twin crystals were observed on the surface of the melt. This is the characteristic feature of $BaTiO_3$ crystals grown by flux method, in which triangular thin plates occur in pairs and join along their common hypotenuse at an acute angle of prism or spine and the spine termination may be either {1 1 1} or {1 1 0} [12]. Generally in as-grown plates of butterfly twin crystals, many laminar *c*- or *a*-domains extend through the crystal

plate having boundaries at an angle of 45° to the major surface [13]. Another type of re-entrant angle crystals were found to grow for Rh concentration of 3 mol%. In this small-angle twinned crystal, one of the spines advanced ahead of the other and a curved re-entrant is formed between two possible {1 0 0} faces. Although this re-entrant probably contributes to the spine development, it is not considered to be as important in controlling the spine growth rate as the re-entrant at the twin plane. The relatively large size of twinned crystal compared to the untwinned one is related to the influence of re-entrant angle type deposition sites on growth rates and ease of formation of two-dimensional nuclei. In this aspect, the re-entrant angle formed by the members of the twinned crystal can be compared to a screw dislocation [12].

Fig. 1 shows polished Rh:$BaTiO_3$ crystals of typical dimension $4 \times 4 \times 2\,mm^3$. Growth runs with faster cooling rate and shorter soaking period resulted in dendritic growth, yielding crystals with flux inclusions. For higher doping concentrations, the flux ratio was increased in order to compensate the decreasing solubility with increasing Rh content. After repeated growth runs, the flux–charge ratio was optimized for each composition as shown in Table 1. The EDX measurements revealed that the dopant concentration in the grown crystals is much lower than the starting composition (Table 1). However, the segregation coefficient is higher than the reported value of 0.01 [10]. Higher level of dopant incorporation is attributed to the step-cooling process, in which the melt is homogenized over a wide range of crystallization temperature, enabling easy movement of solute and dopant material to the crystal grown in the initial stage [14]. No accidental impurities were observed within the detection limit of EDX analysis except a small fraction of platinum due to contamination from the crucible. Addition of more rhodium prevents other accidental impurities being incorporated in the crystal [10]. The optical transmittance of the grown crystals is measured to be in the range 50–60%.

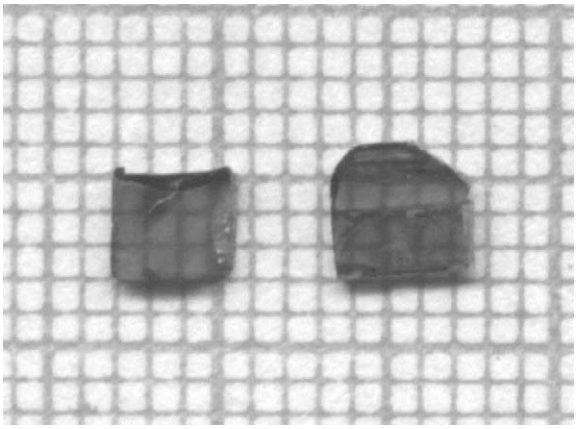

Fig. 1. Polished Rh-doped $BaTiO_3$ single crystals grown from KF flux.

The vein-like structure was observed in the surface of Rh-1 mol%-doped $BaTiO_3$ single crystals by optical microscope. The vein-like structure is formed due to the growth below 1000°C, at a lower supersaturation and low stacking fault energy, as observed generally in $BaTiO_3$ family crystals [15,16]. Concentric spiral growth pattern was observed on the grown crystals for Rh concentration of 3 mol/%. This type of pattern occurs due to the screw dislocation and higher supersaturation [17]. Fig. 2 shows typical ferroelectric domains observed on the crystals grown

Table 1
Growth parameters, crystal composition, lattice parameters for different dopant levels of Rh:$BaTiO_3$ single crystals

Starting composition (mol%)	Flux-charge ratio	Soaking period (h)/ cooling rate (°C/h)	Growth temperature (°C)	Dopant level in the crystals (mol%)	Lattice parameter values	
					a (Å)	c (Å)
$BaTiO_3$:Rh–1.0	75:25	12/3	1170	0.09	3.9753	3.9944
$BaTiO_3$:Rh–3.0	78:22	12/2	1185	0.25	3.9770	3.9928
$BaTiO_3$:Rh–5.0	80:20	15/1	1190	0.45	3.9779	3.9890

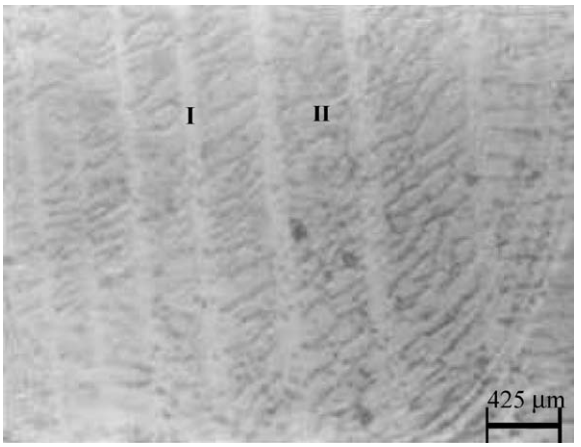

Fig. 2. Domain structure observed in Rh:$BaTiO_3$ (Rh-1 mol%) crystals after etching with HCl. The regions "I" and "II" represent the contrast between domains: the positive domains look "bright" and the negative domains are "dark".

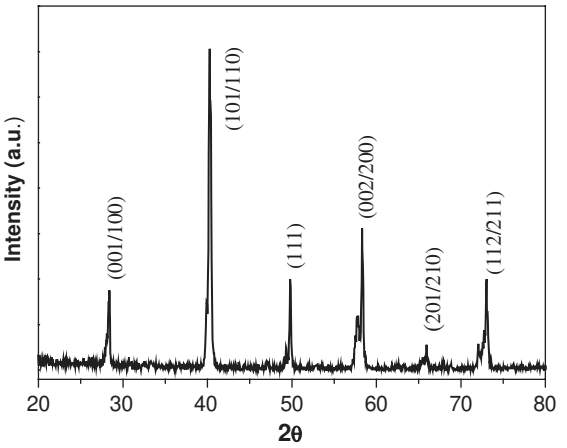

Fig. 3. X-ray diffraction pattern of Rh:$BaTiO_3$ (5 mol% of Rh) crystal. The pattern confirms the tetragonal structure of the grown crystal.

from different Rh concentrations (1 and 3 mol%) after chemical etching using concentrated HCl [18]. The regions "I" and "II" represent the contrast between domains: the positive c^+ domains look "bright" and the negative domains c^- are "dark" [19]. Domain boundaries are distinctly seen with a definite order of the boundaries depending on the crystal orientation.

Fig. 3 shows the powder X-ray diffraction patterns of Rh:$BaTiO_3$ crystals grown from 5 mol% of Rh. The studies confirmed the tetragonal structure of Rh:$BaTiO_3$ with a clear separation between (0 0 2) and (2 0 0) peaks similar to pure $BaTiO_3$ at room temperature [15]. Variation in a- and c-lattice parameters (Table 1) calculated by least square fitting method, reveals that the tetragonality slightly decreases with increasing Rh concentration as the line broadening and c/a ratio of $BaTiO_3$ lattice are highly sensitive to impurities [20]. Laue X-ray pattern (Fig. 4) has been taken for the grown crystal. Sharp and symmetrical spots show the single crystalline nature and four-fold symmetry, which corresponds to tetragonal system. Laue patterns have also been taken in different areas of the same crystal and the homogeneity was confirmed.

Dielectric constant vs. temperature for Rh-doped $BaTiO_3$ single crystals are shown in Fig. 5.

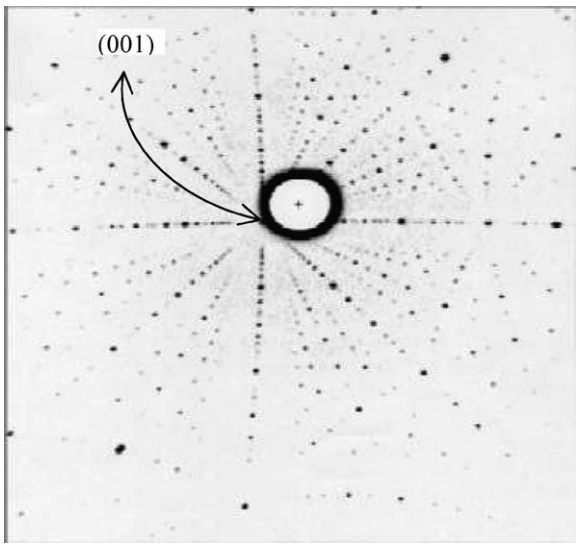

Fig. 4. X-ray Laue pattern taken for Rh:$BaTiO_3$ single crystal.

The Curie temperature (T_c) decreases with increasing Rh concentration. Temperature vs. $1/\varepsilon'$ plots confirm the first-order phase transition and also the values of

$$\frac{d}{dT}\left(\frac{1}{\varepsilon}\right)_{T<T_c} \Big/ \frac{d}{dT}\left(\frac{1}{\varepsilon}\right)_{T>T_c} \text{ are not equal to 2.}$$

The values of Curie temperature, transition temperature and Curie constant for different

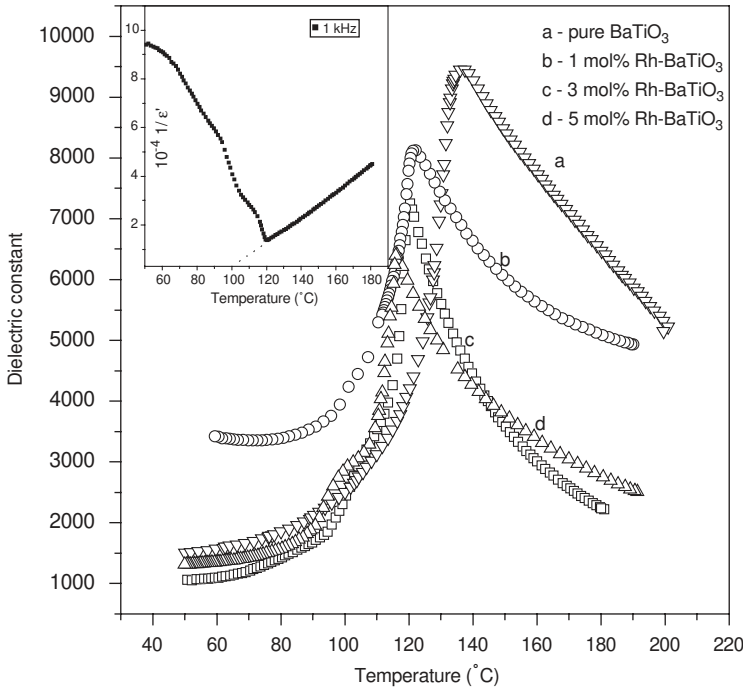

Fig. 5. Dielectric constant vs. temperature for Rh-doped $BaTiO_3$ single crystals measured at a frequency of 1 kHz. The insert shows the $1/\varepsilon$ vs. temperature for 5 mol% of Rh:$BaTiO_3$ crystal.

Table 2
Curie temperature, spontaneous polarization and Curie constant for different dopant concentrations of Rh:$BaTiO_3$ single crystals

Starting composition (mol%)	T_c (°C)	P_s (μC/cm^2)	$C \times 10^4$
$BaTiO_3$:Rh–1.0	121.5	22	9.6248
$BaTiO_3$:Rh–3.0	120.3	20	9.3699
$BaTiO_3$:Rh–5.0	115.9	16	8.8746

concentrations of Rh-doped $BaTiO_3$ crystals are given in Table 2. The change in Curie temperature (T_c) is due to the lattice dimensions change, i.e., volume change, which is equivalent to the change in T_c produced by pressure according to the Clapeyron equation. The dielectric constant increases with a maximum value at the Curie temperature. For higher Rh content, the dielectric constant is measured to be 6500. It is observed that the phase transition is very sharp without diffused nature.

4. Conclusions

Growth aspects of Rh-doped $BaTiO_3$ single crystals have been investigated. The dopant has significant effect on the growth temperature, cooling rate, soaking period and morphology of the grown crystals. Well-defined transparent crystals of size $4 \times 4 \times 2\,mm^3$ have been grown with optimized growth parameters. Though the incorporation of Rh into the crystal is very low compared to the starting composition, the crystals grow without any accidental impurities. The step-cooling process is effective in increasing the segregation of Rh into growing crystal. The decrease in Curie temperature for Rh-doped $BaTiO_3$ crystals is attributed to the decrease in tetragonality. The dielectric constant increases sharply, indicating the absence of diffused phase transition. It is inferred that higher rhodium doping in $BaTiO_3$ yields bulk single crystals with promising ferroelectric

properties, which is useful for near-infrared photorefractive applications.

Acknowledgements

One of the authors (SM) is grateful to the Council of Scientific and Industrial Research (CSIR), Government of India for the award of Senior Research Fellowship.

References

[1] P. Günter, J.-P. Hiugnard (Eds.), Photorefractive Materials and their Applications I, Springer, Berlin, 1988.
[2] S. MacCormack, J. Feinberg, CLEO Tech. Digest 11 (1993) CtuN19.
[3] M. Kaczmarek, G.W. Ross, P.M. Jeffery, R.W. Eason, P. Hribek, M.J. Damzen, R. Ramos-Garcia, R. Troth, M.H. Garrett, D. Rytz, Opt. Mater. 4 (1995) 158.
[4] A. Brignon, J.-P. Huignard, M.H. Garrett, I. Mnushkina, Opt. Lett. 22 (1997) 215.
[5] H. Song, S.X. Dou, M. Chi, H. Gao, Y. Zhu, P. Ye, J. Opt. Soc. Am. B 15 (1998) 1329.
[6] S. Bernhardt, H. Veenhuis, P. Delaye, R. Pankrath, G. Roosen, Appl. Phys. B 72 (2001) 667.
[7] B.A. Wechsler, M.B. Klein, C.C. Nelson, R.N. Schwartz, Opt. Lett. 19 (1994) 536.
[8] X. Xu, Z. Shao, X. Mu, C. Du, Z. Wang, H. Xu, H. Luo, Appl. Phys. Lett. 78 (2001) 569.
[9] M. Kaczmarek, R.W. Eason, Opt. Commun. 154 (1998) 334.
[10] M. Kaczmarek, R.W. Eason, I. Mnushkina, Appl. Phys. B 68 (1999) 813.
[11] X. Xu, Z. Wang, X. Yang, J. Liu, X. Mu, Z. Shao, H. Xu, H. Luo, Appl. Phys. B 73 (2001) 223.
[12] R.C. Devries, J. Am. Ceram. Soc. 42 (1959) 547.
[13] S.I. Hamazaki, F. Shimizu, S. Kojima, M. Takashige, J. Phys. Soc. Jpn. 64 (1995) 3660.
[14] R. Jayavel, C. Sekar, P. Murugakoothan, C.R. Venkateswara Rao, C. Subramanian, P. Ramasamy, J. Crystal Growth 131 (1993) 301.
[15] S. Balakumar, R. Ilangovan, S. Ganesa Moorthy, C. Subramanian, Mater. Res. Bull. 30 (1995) 897.
[16] R. Varatharajan, S. Madeswaran, R. Jayavel, J. Crystal Growth 225 (2001) 484.
[17] O. Marella, B. Molinas, B.B. Fabris, J. Mater. Sci. 29 (1994) 3497.
[18] N.R. Ivanov, N.A. Tikhomirova, A.V. Grinberg, S.P. Chumakova, E.I. Eknadiosyants, V.Z. Borodin, A.N. Pinskaya, V.A. Babonskikh, V.A. Dyakov, Crystallogr. Rep. 39 (1994) 593.
[19] A. Skliar, G. Rosenman, Y. Lereah, N. Angert, M. Tseitlin, M. Roth, Ferroelectrics 191 (1997) 187.
[20] W.R. Buessem, M. Kahn, J. Am. Ceram. Soc. 59 (1971) 458.